Morphology, physical conditions and relation with star formation of filamentary structure identified on Hi-GAL maps of the Galactic Plane

E.Schisano[1,2], K.L.J.Rygl[2], S.Molinari[2], G.Busquet[2], D.Elia[2], M.Pestalozzi[2], D.Polychroni[3], N.Billot[4], S.C.O.Glover[5], A.Noriega-Crespo[1], R.Paladini[1], T.J.T.Moore[6], R.Plume[7], E.Vazquez-Semadeni[8]

(submitted to ApJ)

[1]California Institute of Technology (USA), [2]Istituto di Astrofisica e Planetologia Spaziali (Italy), [3]University of Athens (Greece), [4]Instituto de RadioAstronomia Milimetrica (Spain), [5]Zentrum fur Astronomie, Universtat Heidelberg (Germany), [6]Astrophysics Research Institute, Liverpool (UK), [7]Department of Physics and Astronomy, University of Calgary (Canada)

Abstract: Star-forming molecular clouds have a complex structure with gas and dust often arranged in filaments. Herschel observations, thanks to their previously unmatched resolution and sensitivity, have revealed that the organization of the dense interstellar material into filamentary structures is more recurrent than previously thought. To understand the role filaments play in the process of star formation it is necessary to study a statistical sample in different enviroments. In this poster we present the method we have developed to identify filaments on Herschel maps of the Galactic Plane observed in the framework of the Hi-GAL project. We further discuss the physical properties of the filaments sample identified in the galactic longitude range between l=216.5° to l=225.5° and their relation with the presence/absence of clump formation activity.

1. Introduction

Stars form within molecular clouds. Observations at different wavelengths indicate that the dust and gas in molecular clouds are organized into different morphologies: from single and isolated (Jackson et al. 2010) to groups of parallel filaments (Busquet et al. 2013), from networks of filaments crossing each other (Molinari et al. 2010, Andre'et al. 2010, Arzoumanian et al. 2011, Peretto et al. 2012) to filaments converging into "hub" structures (Meyers 2009, Hill et al. 2011). At all scales, filaments appear to be a key-structure required to build the densities necessary for star formation.

Despite the fact that filaments are found everywhere and are spatially associated with pre/protostellar cores, their effective relation with star formation is still uncertain. Such a question can be answered only through a ***quantitative*** study on a large sample of filaments and the cores/clumps hosted by them over a wide range of spatial scales and physical conditions.

Only the large surveys of the nearby star-forming regions (Gould Belt survey, Andre'et al.2010) and of the Galactic Plane (Hi-GAL, Molinari et al. 2010a) carried out with Herschel, allow such kind of unbiased studies.

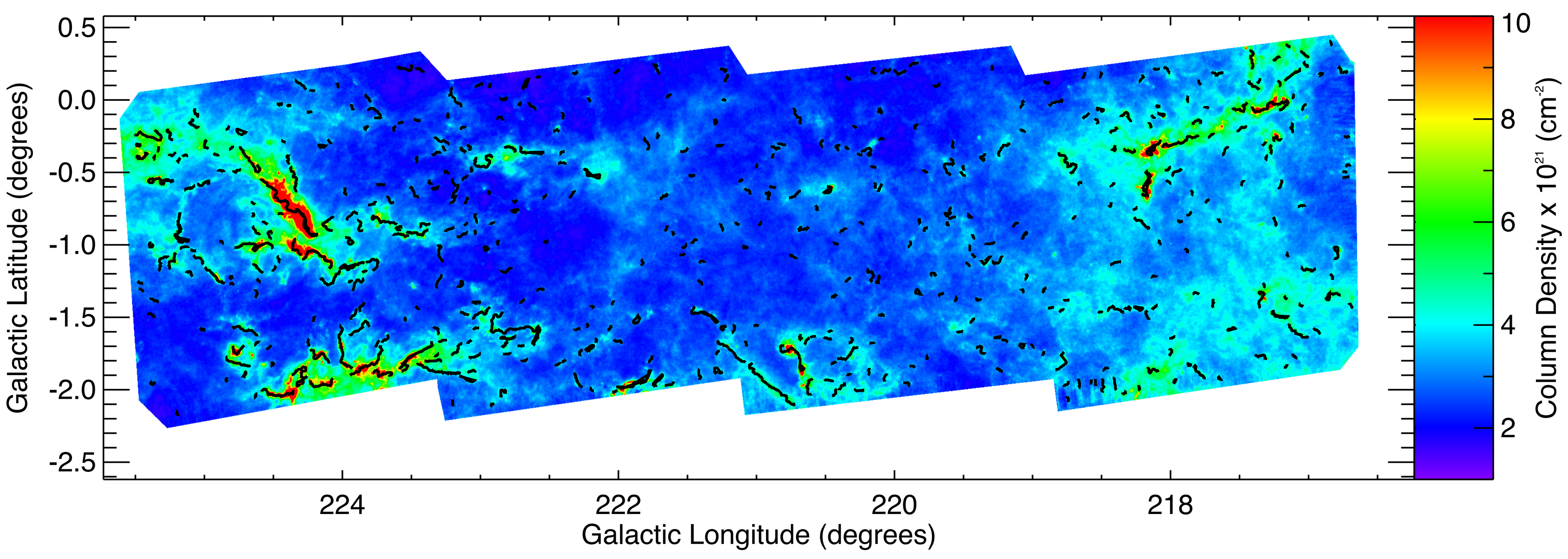

Fig.2 Column density map from Elia et al. 2013 of the Galactic Plane in the Galactic longituted range between l=216.5° and l=225.5°. Data wavelengths 160, 250, 350 and 500 μm were used in the calculation. Maps were smoothed to 36" resolution and sampled on a 11.5" wide pixel. A standard dust opacity law with $k_{250\mu m}$ = 0.1 cm²g⁻¹ and emissivity β=2 was adopted. Black lines show the spines of the filaments identified with a threshold equal to 3 times the σ computed at each location on a 2' wide region.

3. Filamentary structures in the Galactic Plane between l=216.5° and l=225.5°

We applied our method to the column density maps computed from the four *Herschel* Hi-GAL maps in the Galactic longitude range of l=216.5° to l=225.5° presented by Elia et al. 2013 and identified ~500 filaments splitted in ~2000 substructures (see Fig. 2).

We found filaments with lengths as short as ~0.5 pc up to 30 pc and widths between ~0.1 pc up to 3 pc, lying at distance between ~0.5 to 7.5 kpc.

Most of the filaments are resolved in our observations and have a mean width of ~0.5 pc (Fig 3.) larger than previous studies in nearby clouds (Arzoumanian et al. 2011), but in accordance with the filamentary IRDC (Jackson et al 2010). However, we still find that the width is independent from the central density like in Arzoumanian et al. 2011.

All the material with density N_{H2}> 6x10²¹ cm⁻² is arranged into filaments, but <u>such dense matter is not all associated with high density clumps hosted inside the structures</u> (Fig.4).

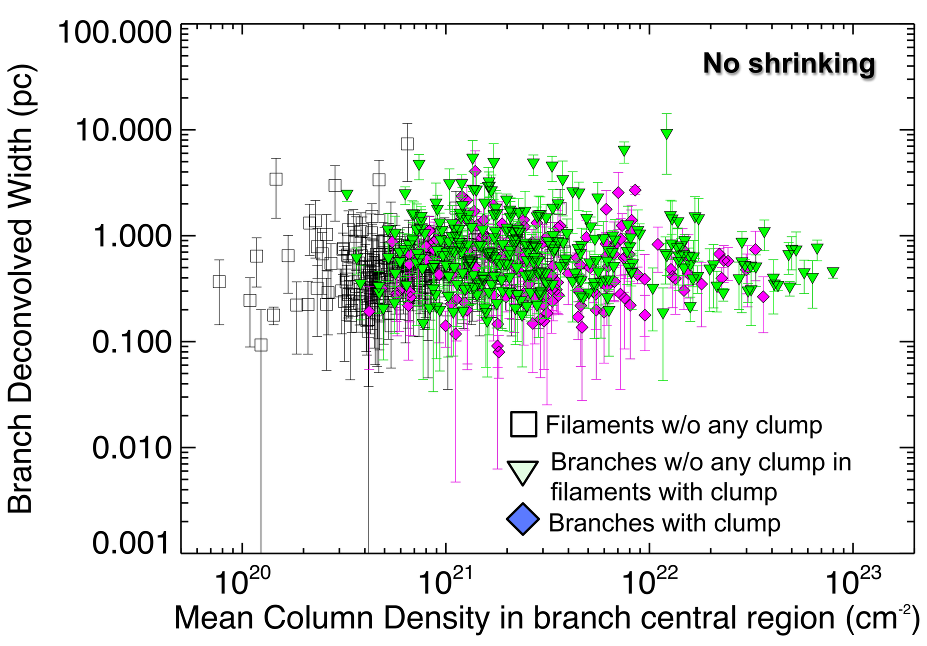

Fig.3: Deconvolved size of the filaments as function of the mean central column density N_{H2}. Sizes are independent from N_{H2}, indicating that it is not setted by self-gravity.

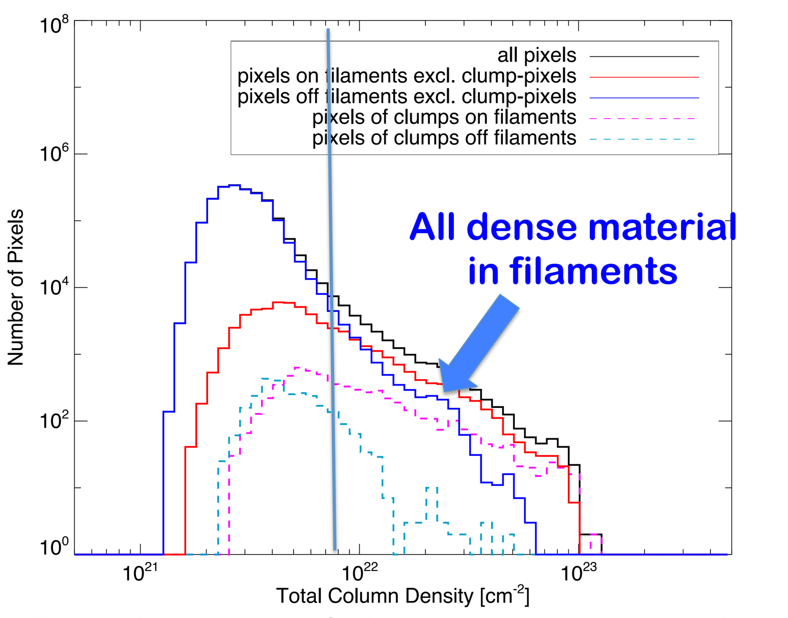

Fig.4: Histogram of the column density splitted following the type of feature on the map. The dense material is concentrate into filaments, but not all concentrated in the hosted clumps.

5. Conclusions

Our unbiased investigation over a large sample of filaments identified on the Galactic Plane in a wide range of physical condition confirms quantitatively that <u>the dense material is almost always arranged into structures that can be defined as filamentary</u>. Furthermore, while it is still possible to find clump formation outside filaments, <u>only in filaments there are the Σ conditions for high-mass star formation</u>. Clumps may form in globally gravitationally subcritical structures, but <u>filaments show an increase of the linear density with time on scales larger than clumps</u>.

Linear density can only increase by accreting from the local surrounding (within the filament itself or from the enviroment), since we do not measure any shrinking of the structure. <u>Most of the filaments are expected to be in a state of dynamical evolution</u>.

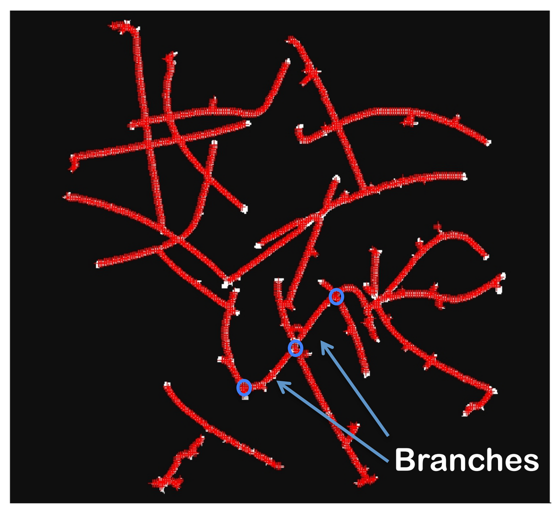

Fig 1: Example of our filament detection. We simulated group of realistic filaments overlayed on portion of a Hi-GAL map used as background (top panel, left). Each filament has brightness variation along the spine as well as simulated compact sources. The map with the minimum negative eigenvalue λ_1 of *H(x,y)* in each pixel (top panel, center) enhances the embedded filamentary structure with respect to the background. The filaments are identified by a proper thresholding of the λ_1 map (top panel right). We marked with a green circle two real filaments identied in the underlying background emission.

The central filament region (the spine) is traced by removing iteratively pixels from both sides of the RoI. The results is shown in red in the bottom panel. The blue circles identify "nodes" along the filament spine, where two or more substructure intersect, in this case due to projection effects. We call branch the portion of the RoI between two nodes.

2. Filaments Detection (basic idea)

We define a filament as a 2-D extended feature, covering a portion of the map, with an elongated, cylinder-like, shape and with a relatively higher brightness contrast with respect to its surrounding. We study the eigenvalues (λ_1,λ_2) of the Hessian Matrix, *H(x,y)*, of the map, *I(x,y)* to trace the features defined above since:

-) cylinder-like shapes have a particular "fingerprint" in the curvature along their axis, with a stronger concavity along one direction than the orthogonal one.
The *H(x,y)* is proportional to the curvature and its eigendirections (A_1, A_2) immediately trace the principal directions where the difference in curvature is the largest.

The central region of the filaments have: $\lambda_1 << \lambda_2$ (Bond et al. 2010)

-) the second derivate measures the variation of the gradient of *I(x,y)*, i.e. its change in contrast, hence its thresholding give a first rought estimate for the filament's edges.

The whole filamentary region have: $\lambda_1 < 0$

We tested the performance of our method on simulated filaments of different length, thickness, crowdness and constrast with respect the background, overlayed over real Herschel observations of the ISM emission (see Fig.1). We found that filament properties are recovered to within a 20% uncertainty with respect to input values, unless the filament/background contrast is too low. Details on the detection method are presented in Schisano et al. 2013, submitted.

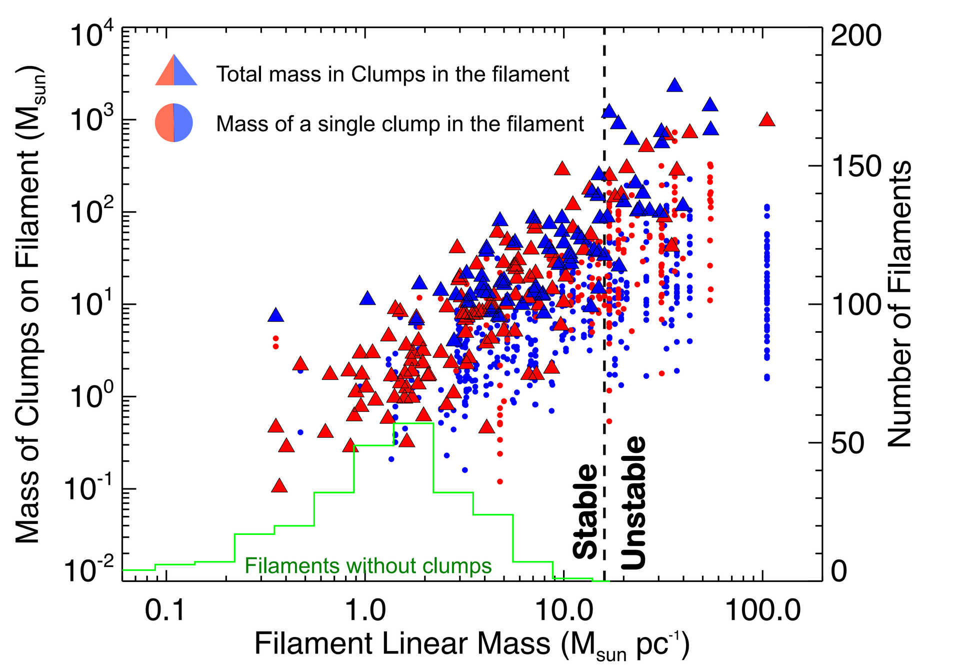

Fig.5: Mass of the hosted clumps as function of the average filament m_{lin}, given by the total mass of the filament divided for its length.

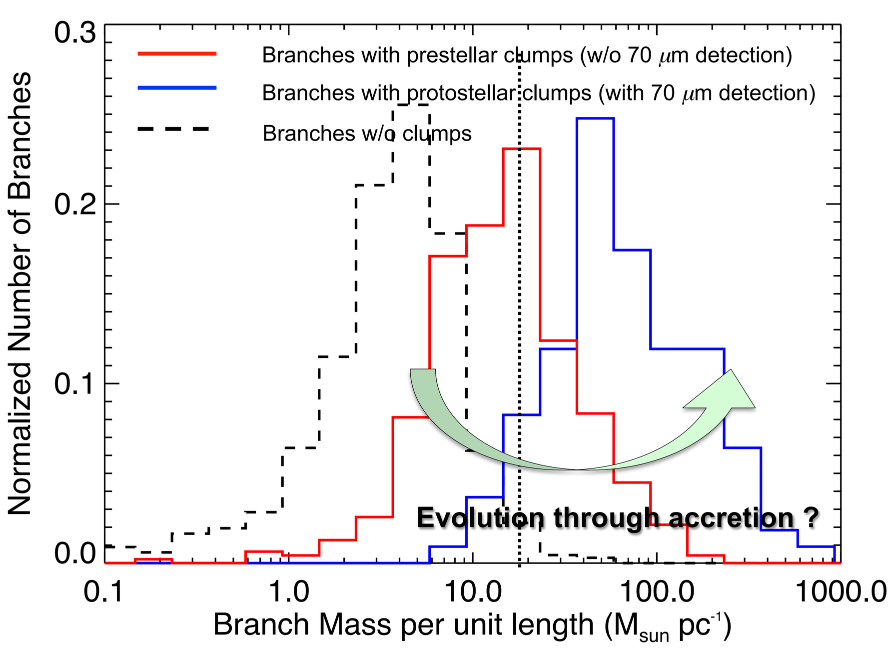

Fig.6: Histograms of the local m'_{lin} in the filament, given by the branch mass divided its length.

4. Filaments and the relation with star formation

We studied the properties of the clumps identified by Elia et al.2013 comparing with the properties of our filament sample in the same.

We found that most of the clumps (74%) are associated with filaments. the local density enhancements necessary to trigger high-mass star formation (Σ~1 g cm⁻²; Krumholz & McKee 2008) are only found within filaments (see Polychroni et al. 2013).

For each filament we assigned a global linear density, or average mass per unit length, m_{lin}, and a local m'_{lin} computed in the branches. All the filaments without clumps have m_{lin} < 10 M_{sun}pc⁻¹, less than the critical value of ~16 M_{sun}pc⁻¹ necessary for support of the structure against its own gravity. Filaments hosting clumps have m_{lin} between 1 and 90 M_{sun}pc⁻¹. <u>Higher m_{lin} filaments appear to channel more mass into compact clumps, forming more massive single clumps than lower m_{lin} filaments</u> (Fig. 5).

We found global subcritical filaments might still host star formation as in Hernandez & Tan 2011. However, locally, all the regions hosting *active star formation* (protostellar clumps) have m'_{lin} above the critical value (Fig. 6).

References: **Andre',P.** et al.,2010, A&A, 518, L102; **Arzoumanian,D.** et al.2011,A&A, 529, L6; **Bond, N.A.**, 2010, MNRAS, 409, 156; **Busquet, G.**, et al., 2013, ApJ, L26; **Elia, D.**, et al.,2013, ApJ, 772, 45; Hernandez, A.K. & Tan, J.,C., 2011, ApJ, 2011, 730, 44; **Hill, T.**, et al., 2011, A&A, 533, A94; **Jackson, J.M.**, 2010, ApJ, 719, L185; **Krumholz, M., & McKee**, C.F., 2008, Nature, 451, 1082; **Meyers, P.C.**, 2009, ApJ, 700, 1609; **Molinari, S.**, et al., 2010a, PASP, 122, 314; **Molinari, S.**, et al., 2010, A&A, 518, L100; **Peretto, N.**, et al., 2012, A&A, 541, A63; **Polychroni, D.**, et al. 2013, A&A accepted.